

# AIRBORNE SOIL MOISTURE DETERMINATION USING A DATA FUSION APPROACH AT REGIONAL LEVEL

*Francisco Martín<sup>1</sup>, Juan Fernando Marchan<sup>1</sup>, Albert Aguasca<sup>2</sup>, Mercedes Vall-Ilossera<sup>2</sup>, Jordi Corbera<sup>1</sup>, Adriano Camps<sup>2</sup>, Maria Piles<sup>3</sup>, Luca Pipia<sup>4</sup>, Anna Tardà<sup>4</sup>, Alberto G. Villafranca<sup>1</sup>*

<sup>1</sup> Catalan Earth Observation Program – Institut Cartogràfic de Catalunya

<sup>2</sup> Remote Sensing Lab – Universitat Politècnica de Catalunya and IEEC/CRAE-UPC

<sup>3</sup>SMOS Barcelona Expert Center, Pg. Marítim de la Barceloneta 37-49, 08003 Barcelona, Spain

<sup>4</sup> Remote Sensing Area – Institut Cartogràfic de Catalunya

## ABSTRACT

HUMID is a regional level airborne soil moisture mission. The envisioned product combines two key characteristics. On one hand, it provides robustness in presence of surface roughness and vegetation. On the other hand, it improves the current spatial resolution offered by L-band radiometers using a data fusion approach, where the data from an L-band radiometer developed by the Remote Sensing Lab at the Universitat Politècnica de Catalunya will be combined with data from a thermal and a VNIR hyperspectral sensors from the Institut Cartogràfic de Catalunya.

**Index Terms**—Soil moisture, data fusion, microwave radiometry, VNIR, vegetation indexes, surface temperature

## 1. INTRODUCTION

Water cycle is a capital Earth System process, affecting significantly the continuous exchange of moisture –powered by the energy from the Sun– between oceans, atmosphere and lands. Soil moisture (SM) is a key factor in the water cycle, controlling the exchange of water and heat between the land surface and the atmosphere through evaporation and plant transpiration. Therefore, since SM is related to temperature, humidity and precipitation, its retrieval can significantly improve current meteorological forecasts and hydrological models. Consequently, ESA and NASA have started dedicated missions to study this variable. In November 2<sup>nd</sup>, 2010 ESA launched SMOS (Soil Moisture and Ocean Salinity) mission, and NASA has scheduled the launch of SMAP (Soil Moisture Active and Passive) for November of 2014. However, both SMOS and SMAP missions are designed for global applications, focusing mainly on a better understanding of climate change.

In this scenario PCOT (Catalan Earth Observation Program), as a supporting center of the ICC (Institut Cartogràfic de Catalunya) has identified slightly different

end-user needs at local/regional level with respect to those required at global level. Thus, HUMID aims for recovering SM at these regional scales, where spatial resolution and accuracy are paramount issues of the end product.

Following the ideas proposed to disaggregate SMOS pixels using MODIS VNIR data [1], HUMID is based on a data fusion process, combining a thermal and VNIR hyperspectral sensors with an L-band radiometer. This radiometer has been designed and manufactured by the Remote Sensing Lab (RS\_Lab) of the Universitat Politècnica de Catalunya (UPC) (Fig. 1).



*Figure 1. Thermal and VNIR hyperspectral sensors and radiometer installation onboard ICC airplane*

## 2. DATA

The results presented in this paper are based on the flight campaign conducted by ICC over the area of Gimenezells (Lleida, 41°39'21.34'' N, 0°24'21.25'' E) on March 31<sup>st</sup>, 2011. The area has a Calcixerolic Xerochript soil with loam texture, where different types of covers are present, from bare soil to forest soils. The predominant vegetated areas are

fields of alfalfa, cereals, vineyards and fruit trees. The atmospheric conditions during the flight were optimal (sunny day with few clouds). Some 8 days prior to the measurements strong downpours (~60 mm) took place all over the area.

Two photogrammetric windows of ICC airplane Cessna 208 Caravan were used to simultaneously acquire TIR and VNIR data (window 1) and L-band brightness temperature (window 2).

The L-band radiometer (ARIEL-2) has a seven patch antenna array designed to match the aircraft's photogrammetric windows ( $\phi = 50$  cm), with a half power beamwidth (HPBW) of  $25^\circ$  and a radiometric accuracy of 1 K. ARIEL-2 is the second version of the ARIEL-1 radiometer prototype [2] developed for small remote controlled aircrafts, and includes an internal cold load for improved calibration. As ARIEL-1, it has a single nadir-looking beam and a single polarization (horizontal). Future cooperation between ICC and UPC can result in more advanced configurations to obtain bi-angular and/or bi-polarization data.

The flight plan consisted of 4 strips, 3 in North-South direction and spaced 100-120 m (overlapping with each other) and a 4<sup>th</sup> transversal to these ones. The altitude of the flight was 1121 meters, thus providing a radiometer spatial resolution between 250 and 300 meters, and VNIR and thermal spatial resolutions of 2 m. In addition to the flight measurements, a ground truth campaign was carried out. SM measurements (Decagon EC\_5) and temperature measurements were acquired on seven representative spots, along with soil samples for further analysis (Fig. 2).



Figure 2. Flight Plan and ground truth over selected area

### 3. THEORETICAL BASIS

The goal of the HUMID program is to remotely retrieve SM. Water has a strong influence in the overall dielectric constant, which in turns affect the surface emissivity, and thus its brightness temperature:

$$e_{gp} = \frac{T_{Bp}}{T_{phys}}, \quad (1)$$

where  $e_{gp}$  is the emissivity, which is one minus the Fresnel Reflectivity ( $\Gamma_{gp}$ ),  $T_B$  is the brightness temperature and  $T_{phys}$  is the physical temperature. Nonetheless, brightness temperature is affected by the presence of roughness and vegetation. Therefore, it is necessary to account for it in the geophysical model. Roughness can be modeled by modifying the Fresnel reflectivity expression, as proposed in [3],

$$\Gamma_{gp} = \left( (1 - QR)\Gamma_{bp} + QR\Gamma_{bp} \right) \exp(-HR \cos^{Np}(\theta)), \quad (2)$$

where QR is the polarization coupling factor related with the polarization mixing that can be induced due to the roughness, HR is an adimensional effective surface roughness, and Np is an integer used to parameterize the dependence that presents the roughness depending on the SM.

Vegetation is parameterized using the tau-omega model [4]:

$$T_{Bp} = (e_{gp})T_g\gamma_p + (1 - w_p)T_c(1 - \gamma_p) + (1 - e_{gp})(1 - w_p)T_c(1 - \gamma_p)\gamma_p, \quad (3)$$

$T_g$  is the effective soil temperature,  $T_c$  is the vegetation temperature,  $w_p$  is the single scattering albedo (parameterizes the scattering effects within the canopy layer). Finally,  $\gamma_p$  is the transmissivity of the vegetation, which is related to the optical depth and thus with the vegetation attenuation properties:

$$\gamma_p = \exp(-\tau_p / \cos\theta), \quad (4)$$

where  $\tau_p$  is the optical depth. It can be linearly related to the Vegetation Water Content (VWC) using the  $b_p$  parameter, which depends on the structure and the type of vegetation [5].

## 3. MODEL

### 3.1. Radiometric soil moisture retrieval

The first step for the moisture retrieval is to recover the SM at the radiometer resolution, i.e. 250-300 m. This coarse resolution will be further improved in the subsequent data

fusion procedure. Subsequently, a Cost Function minimization process, involving both measured and estimated radiometer brightness temperatures, takes place to retrieve SM. The soil dielectric constant is computed by applying the Dobson model [6, 7] and the Peplinki's formulation [8, 9] to estimate  $T_b$  (direct model). Then, the Fresnel reflection [10, 3] is computed. Eventually the tau-omega model is applied to estimate  $T_b$  [4]. This estimated  $T_b$  not only depends on SM, but also on soil texture, surface temperature, roughness level, and vegetation cover.

TASI, the thermal hyperspectral sensor, retrieves surface temperature, whereas the effective surface roughness will be considered as constant throughout the scene. Additionally, the single scattering albedo is assumed to be 0, since at L-band it can be neglected in many cases. Also, soil texture is taken as 50% sand and 20% clay. Silt has been used for the remaining 30%.

The optical depth will be derived from the Leaf Area Index (LAI) using the SMOS ATBD relationship :

$$\tau = b' LAI + b'' , \quad (5)$$

where  $b'$  is equal to 0.06 and  $b''$  to 0.

LAI is not directly available as an input, but several studies [11-15] relate vegetation indexes with LAI. Therefore, considering the availability of LAI and NDVI MODIS products over the considered area – which present a correlation of  $R^2 = 0.85$  – a semi-empirical relationship is derived:

$$LAI = 0.1251 \exp (3.8804 \cdot NDVI) , \quad (6)$$

Hence, LAI is derived from the NDVI obtained with CASI (VNIR hyperspectral sensor), and so optical depth can be incorporated into the model.

### 3.1. Data fusion approach

The data fusion approach here presented is based on the modification of the Carlson 'Triangle method'[16] proposed on [1], where the L-band brightness temperature is included to increase the radiometric accuracy of the method proposed by Carlson:

$$sm = \sum_{i=0}^n \sum_{j=0}^m \sum_{k=0}^o a_{ijk} NDVI^i T_s^j T_B^k \quad (7)$$

## 4. RESULTS

The next results are focused on a subarea with UTM coordinates ( $x = 284200-284600$ ,  $y = 4616000-4608000$ ) to analyze better the results.

Figure 3 it shows the data employed to derive the soil moisture: brightness temperature, surface temperature and NDVI.

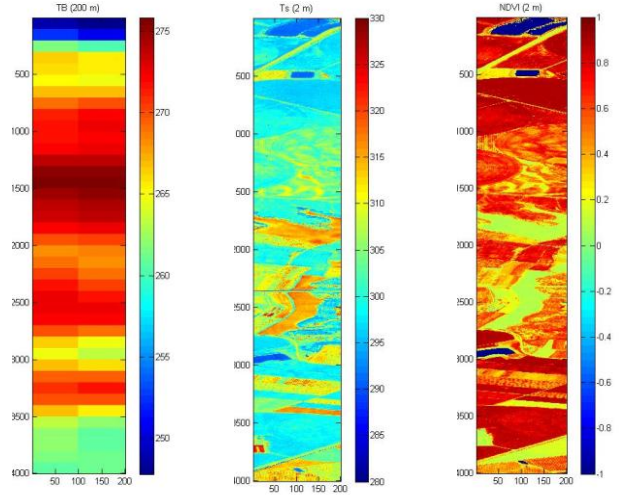


Figure 3. (a)TB , (b)Ts (c)NDVI.

Figure 4 shows the soil moisture derived at the radiometric scale, and after applying the Carlson method including the brightness temperature.

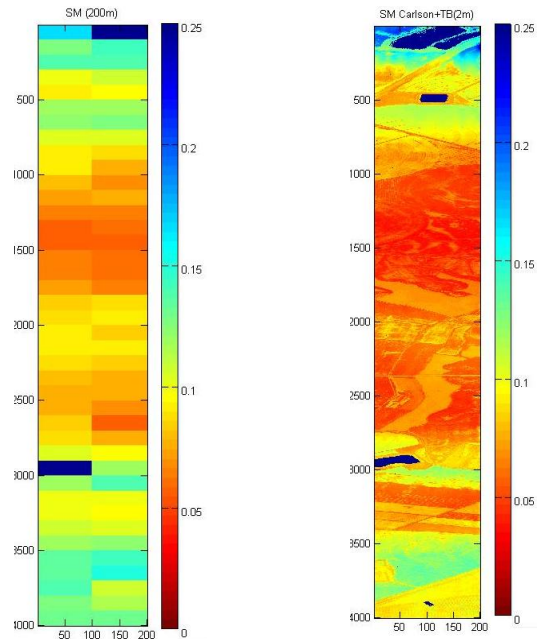


Figure 4(a) Soil moisture at radiometric resolution, (b) Downscaled soil moisture.

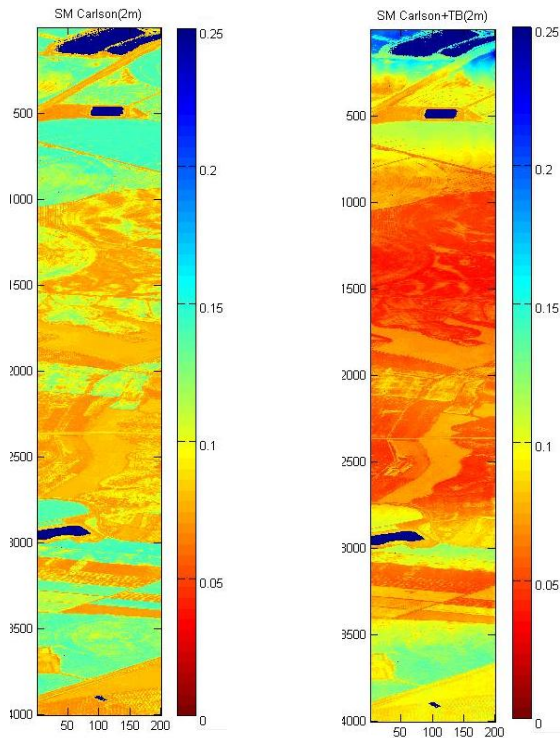


Figure 5. (a) Soil moisture derived applying Carlson method, (b) Soil moisture adding the Tb in the Carlson method

Figure 4 shows the high spatial resolution achieved after applying the modified Carlson method, whereas fig 5 shows how the soil moisture derived from the modified Carlson method has a higher radiometric resolution.

#### 4. CONCLUSIONS

The flight campaign over selected area has been carried out successfully. Thermal, VNIR and radiometer sensor data have been correctly captured. The preliminary results of recovery SM from Tb are in accordance with preliminary data from ground truth.

The chosen data fusion approach to perform pixel disaggregation has been applied to the data. Airborne soil moisture determination using data fusion approach at regional level seems at hand in the near future.

#### 11. REFERENCES

[1] Piles. M., Camps. A., Vall-llossera. M., Corbella. I., Panciera. R., Rüdiger. C., Kerr. Y., Walker. J., "Downscaling SMOS-derived soil moisture using MODIS visible/infrared data", *IEEE Transactions on Geoscience and Remote Sensing*, 2011.  
 [2] Acevo-Herrera, R.; Aguasca, A.; Bosch-Lluis, X.; Camps, A.; Martínez-Fernández, J.; Sánchez-Martín, N.; Pérez-Gutiérrez, C. Design and First Results of an UAV-Borne L-Band Radiometer for Multiple Monitoring Purposes. *Remote Sens.* 2010, 2, 1662-1679.

[3] Wang, J. R., & Choudhury, B. J., "Remote sensing of soil moisture content over bare field at 1.4 GHz frequency", *Journal of Geophysical Research*, 86, pp. 5277-5282, 1981.  
 [4] Mo, T., Choudhury, B. J., Schmugge, T. J., Wang, J. R., & Jackson, J. T., "A model for microwave emission from vegetation-covered fields", *Journal of Geophysical Research*, 87(11), pp. 229-237, 1982.  
 [5] Jackson, T. J., & Schmugge, T. J., "Vegetation effects on the microwave emissions of soils", *Remote Sensing of Environment*, 36, pp. 203-212, 1991.  
 [6] Dobson, M. C., Ulaby. F. T., Hallikainen. M. T., & Elrayes. M. A., "Microwave Dielectric Behavior of Wet Soil .2. Dielectric Mixing Models", *IEEE Transactions on Geoscience and Remote Sensing*, vol. 23, pp. 35-46, 1985.  
 [7] Hallikainen. M. T., Ulaby. F. T., Dobson. M. C., Elrayes. M. A., & Wu. L. K., "Microwave Dielectric Behavior of Wet Soil .1. Empirical-Models and Experimental Observations", *IEEE Transactions on Geoscience and Remote Sensing*, vol. 23, pp. 25-34, 1985.  
 [8] Peplinski. N. R., Ulaby. F. T., & Dobson. M. C., "Dielectric Properties of Soils in the 0.3-1.3-GHz Range", *IEEE Trans Geosci. Remote Sens.*, vol. 33, pp. 803-807, 1995.  
 [9] Peplinski. N. R., Ulaby. F. T., & Dobson. M. C., "Corrections to "Dielectric Properties of Soils in the 0.3-1.3- GHz Range", *IEEE Trans Geosci. Remote Sens.*, vol. 33, pp. 1340, 1995.  
 [10] F. T. Ulaby, R. K. Moore, and A. K. Fung, *Microwave Remote Sensing - Active and Passive*, vol. 1. Norwood, USA: Artech House, 1981.  
 [11] Broge. N. H., Leblanc. E., "Comparing prediction power and stability of broadband and hyperspectral vegetation indexes for estimation of green leaf", *Remote Sens of Environment.*, vol. 76, pp. 156-172, 2000.  
 [12] Xiao. X., He. L., Salas. V., Moore. B., Zha. R., Froelking. S., & Boles. S., "Quantitative relationships between field measured leaf area index and vegetation index derived from VEGETATION images for paddy rice fields", *Int. J. Remote Sens.*, vol. 23, pp. 3595-3604, 2002.  
 [13] Gong. P., Pi. R., Biging. G.S., Larneu. M. R., "Estimation of Forest Leaf Area Index Using Vegetation Indices Derived from Hyperion Hyperspectral Data", *IEEE Transactions on Geoscience and Remote Sensing*, vol. 41, pp. 1355-1362, 2003.  
 [14] Tan. C., Huang. W., Liu. L., Wang. J., Zhao. C., "Relationship between Leaf Area Index and Proper Vegetation Indices across a wide range of cultivars", *IEEE*, pp. 4070-4072, 2004.  
 [15] Haboudane. D., Miller. J. R., Pattey. E., Zarco-Tejada. P. J., Strachan. I. B., "Hyperspectral vegetation indices and novel algorithms for predicting green LAI of crop canopies: Modeling and validation in the context of precision agriculture", *Remote Sensing of Environment*, 90, pp. 337-352, 2004.  
 [15] Carlson. T., "An Overview of the "Triangle Method" for Estimating Surface Evapotranspiration and Soil Moisture from Satellite Imagery", *Sensors*, 7, pp. 1612-1629, 2007.